Sodium electrochemical deintercalation and intercalation in O3-NaRhO2 and P2-NaxRhO2 layered oxides

Louisiane Verger, Marie Guignard, Claude Delmas

Sodium Electrochemical De-intercalation and Intercalation in O3-$NaRhO_2$ and P2-Na_xRhO_2 Layered Oxides.

Louisiane Verger†, Marie Guignard*, and Claude Delmas

CNRS, Université de Bordeaux, Bordeaux INP, ICMCB UMR 5026, 33600 Pessac, France.

ABSTRACT: Sodium transition metal layered oxides are a class of materials which exhibits fascinating properties, such as high thermoelectric power. Whereas most of the work conducted so far focused on 3d transition metals, mainly cobalt, compounds with 4d metals could be excellent materials to obtain new strongly correlated electron systems. This work is focused on Na_xRhO_2 compounds, with O3- and P2-type structures. The P2-type structure was obtained by ion exchange from the potassium phase P2-$K_{0.62}RhO_2$. This type of synthesis was conducted here for the first time on layered oxides with 4d transition metals. The phase diagram of both structures was explored by sodium electrochemical deintercalation/intercalation in a battery. The existence of single phases was shown with presumably different physical properties. As an example, the O'3-$Na_{1/2}RhO_2$ compound electrochemically obtained for the first time exhibits a metallic behavior whereas the O3-NaRhO2 phase is a semiconductor. The synthesis of each single phase existing in both the O3- and P2-type systems should lead to new insights into the structure-properties relationships of this class of materials.

1. INTRODUCTION

Sodium layered oxides with the general formula Na_xMO_2 (where x is comprised between 0 and 1 and M is transition metal) have been intensively studied recently to be used as positive electrode in sodium-ion batteries. Moreover, some of these phases, especially in the Na_xCoO_2 system, exhibit exceptional physical properties such as superconductivity,[1] high thermoelectric power,[2] and metal-insulator transitions.[3] Whereas the Na_xMO_2 systems where M is a 3d element have already been intensively investigated with M = Ti, V, Cr, Mn, Fe, Co and Ni, only few studies report on Na_xMO_2 phases, where M is a 4d element. Layered structures have been reported for Na_xMO_2 systems with M = Nb, Mo, Rh and Ru,[4-7] and sodium electrochemical (de-)intercalation has been realized in a sodium battery for Na_xMO_2 systems with M = Nb, Mo and Rh.[8-10] Also interesting, superconductivity has been discovered in several compositions in the Na_xNbO_2 system.[11] More recently, the Na_xRhO_2 system has drawn more attention. Density functional theory calculations have been used to investigate the thermoelectric properties of several phases in the Na_xRhO_2 system and this computational work has shown that high thermoelectric power could be achieved in different phases.[12] The synthesis of $NaRhO_2$ was first reported as a polycrystalline powder,[7] and then as single crystals.[13] Structure determination from single crystal diffraction has shown that $NaRhO_2$ crystallizes in α-$NaFeO_2$ layered structure-type.[13] This structure-type corresponds to the O3-type in Delmas's nomenclature which is now widely used to describe the different structure-types existing for sodium layered oxides.[14] In this structure, $(RhO_2)_n$ layers are formed by RhO_6 edge-sharing octahedra and sodium ions occupy octahedral interstitial sites between two successive $(RhO_2)_n$ layers.

The phase diagram in the O3-Na_xRhO_2 system has already been studied using different techniques. It was first investigated for sodium contents x comprised between 0.4 and 1 by sodium electrochemical de-intercalation.[10] A few compositions (x = 0.7 and x = 0.85) were then obtained by solid state synthesis at high temperature and the different sodium contents were achieved by increasing the duration of the heat treatment to promote the sodium loss.[15] Very recently, several Na_xRhO_2 phases with sodium content x comprised between 0.25 and 1 were obtained by chemical de-intercalation.[16] Iodine, used as an oxidizing agent, was dissolved in acetonitrile to react with single crystals of $NaRhO_2$.

All these works have shown that the O3-type structure was preserved for all the compositions in the Na_xRhO_2 system. No gliding of the $(RhO_2)_n$ layers occurs during the sodium de-intercalation that would give rise to a P3-type structure with trigonal prismatic environments for the remaining sodium ions. This gliding has been observed in other Na_xMO_2 systems with M = Co, Cr or Ni.[17-20]

In this work, we report on a new investigation of the phase diagram in the O3-Na_xRhO_2 system by sodium electrochemical de-intercalation in a sodium battery. We believe that the first investigation performed by electrochemistry was dominated at high voltage by the electrolyte decomposition. We also report on the first synthesis of a Na_xRhO_2 phase with the P2-type structure, obtained by an ion exchange from the potassium layered oxide P2-K_yRhO_2.

2. EXPERIMENTAL SECTION

2.1. Synthesis

O3-$NaRhO_2$ phase was synthesized by solid state reaction from a mixture of sodium carbonate Na_2CO_3 (purity above 99.9%) and rhodium sesquioxide Rh_2O_3 (purity above

99.8%) with a 5 % weight excess of Na_2CO_3, at 900 °C in air for 12 hours in a gold crucible.

For sodium layered oxides with the formula Na_xMO_2, P2-type structures usually exist for a sodium content of approximately 0.7.[14] We firstly tried to obtain the P2-type structure by direct reaction between sodium carbonate Na_2CO_3 and rhodium sesquioxide Rh_2O_3 in stoichiometric conditions to target $Na_{0.7}RhO_2$ (the same precursors as those used for the synthesis of O3-$NaRhO_2$ were used). The reaction was performed at 900 °C during 12 h, under an O_2 flow. A phase with an O3-type structure was obtained. Another attempt was to start from the precursors O3-$NaRhO_2$ and rhodium dioxide RhO_2 (purity above 98 %) in stoichiometric conditions to target $Na_{0.7}RhO_2$, as already successfully done on P2-$Na_{0.71}VO_2$.[21] The precursors were ground together in a glove-box and loaded in a gold tube. The mixture was then heated at 800 °C during 24 h in the gold tube sealed under argon. Two phases with the O3-type structure were this time obtained.

As it was not possible to obtain any P2-Na_xRhO2 phases by direct solid state reaction at high temperature, we tried to synthesize these phases by ion exchange from a potassium layered oxide K_yRhO_2 which can be obtained with a P2-type structure.[22] P2-K_yRhO_2 was synthesized by solid state reaction of a stoichiometric mixture of potassium carbonate K_2CO_3 (purity above 99.99%) and rhodium sesquioxide Rh_2O_3 with the molar ratio 0.6:1 in an O_2 atmosphere at 900 °C for 12 h in a gold crucible. The product was found to be a mixture two P2-K_yRhO_2 phases having different potassium contents. The product was then ground again in a glovebox and heated again in an O_2 atmosphere at 900 °C for 12 h to homogenize the composition of the particles. Potassium hydroxide KOH was added to the mixture (0.2 moles of KOH per mole of Rh_2O_3 used in the first step of the synthesis) to compensate potassium loss by evaporation. Chemical analysis conducted by electron microprobe with ~ 1 μm^3 probe size (CAMECA SX 100) showed that the sample was homogeneous and the phase P2-K_yRhO_2 was found to have the average composition $K_{0.62\pm0.03}RhO_2$.

During the synthesis of P2-$K_{0.62}RhO_2$, an O3-$NaRhO_2$ phase was systematically obtained as an impurity. It appeared that an amorphous impurity containing sodium was present in several commercial batches of rhodium oxide that has been used for all the syntheses. Commercial rhodium oxide was purified before being used for the synthesis of the P2-$K_{0.62}RhO_2$ phase. The purification process consisted in dissolving Rh_2O_3 in a molten salt (equimolar mixture of potassium pyrosulfate $K_2S_2O_7$ and potassium chloride KCl) by heating the mixture at 550 °C in air for 1 hour. After solidification, the mixture was dissolved in boiling distilled water. Rhodium hydroxide $Rh(OH)_3$ was precipitated from this boiling solution (the solution was transparent red) by adding an ammonia solution $NH_{3\,(aq)}$. The yellow precipitate was filtered, amply rinsed and calcinated at 900 °C in air for 1 hour. Pure rhodium sesquioxide Rh_2O_3 was obtained after this process and it was used to synthesize the pure single phase P2-$K_{0.62}RhO_2$.

The second step of the synthesis of the P2-Na_xRhO_2 phase consisted in an ion exchange of potassium by sodium in the P2-$K_{0.62}RhO_2$ phase. A mixture of P2-$K_{0.62}RhO_2$ and sodium iodide NaI (0.73 moles of NaI per mole of P2-$K_{0.62}RhO_2$) was ground in a glovebox. The powder was then pressed in a pellet and it was heated at 200 °C for 24 h in a glass tube sealed under vacuum. The resulting product was washed with anhydrous acetonitrile in a glovebox in order to wash away the potassium iodide KI which was formed during the ion exchange and possibly unreacted sodium iodide NaI. Chemical analysis conducted by electron microprobe indicated that nearly all potassium was exchanged by sodium. Traces of potassium (1 % atomic) were found along with traces of iodine indicating that potassium was present in the resulting powder due to the presence of unwashed potassium iodide KI. The phase P2-Na_xRhO_2 was found to have the average composition $Na_{0.70\pm0.03}RhO_2$.

2.2 X-ray powder diffraction

Laboratory based X-ray powder diffraction measurements (Cu-source Panalytical X'Pert Pro) were performed on Na_xRhO_2 samples in sealed glass capillaries (0.2 mm diameter). High resolution X-ray powder diffraction data for $Na_{1/2}RhO_2$ were collected at the Materials Science and Powder Diffraction (BL04-MSPD) beamline of the Alba synchrotron using a wavelength of 0.8254(2) Å, in the 0-72° 2θ range with a 0.006° step. The powder was loaded in a sealed 0.8 mm diameter Kapton capillary. Structure refinements using the Rietveld method were carried out using TOPAS program.

2.3 Electrochemical characterization

Electrochemical characterization was undertaken in 2032 type coin cells with the following electrochemical arrangement: Na | $NaPF_6$ (1M) in PC (propylene carbonate) + 2% FEC (fluoroethylene carbonate) | Na_xRhO_2 phases mixed with graphite + carbon black powder (Strem Chemicals) and PTFE (polytetrafluoroethylene) as binder (88: 10: 2 weight ratio). The batteries were assembled in a glovebox and cycled using a Biologic VMP3 potentiostat at 25 °C in a temperature-controlled room. Galvanostatic cycling was performed at C/100 rate (1 Na^+ per formula unit (de)intercalated in 100 h) between 2.5 V and 3.8 V.

The electrochemical synthesis of O'3-$Na_{1/2}RhO_2$ was realized in a sodium battery with the following electrochemical chain: metal Na | $NaPF_6$ (1M) in PC (propylene carbonate) + 2% FEC (fluoroethylene carbonate) | O3-$NaRhO_2$. The O3-$NaRhO_2$ compound was used as the positive electrode either as a sintered pellet or as a powder mixed with a graphite/carbon-black powder to improve its electronic conductivity. The batteries were galvanostatically charged at the C/100 rate (1 e^- per rhodium transferred in 100 hours) up to 3.42 V that corresponds to the Fermi level (vs. the Na^+/Na couple) for O'3-$Na_{1/2}RhO_2$. This voltage was determined from the galvanostatic cycling curve. Once this voltage was reached, it was continuously applied to the electrochemical cell. The current was measured during the potentiostatic charge. When it drops down to zero it means that the expected material is obtained. After the charge, the pellet or the powder was recovered, washed with dimethyl carbonate and dried under vacuum.

2.4. Physical characterizations

For transport measurements, sintered pellets of O3-$NaRhO_2$ and pellets of O'3-$Na_{1/2}RhO_2$ obtained by sodium de-intercalation were used in an air-tight apparatus and the electrical resistance was measured using the four-probe technique in the 77-300 K temperature range. The resistance of the pellet was measured while it was continuously heated up.

3. RESULTS AND DISCUSSION

3.1. O3-$NaRhO_2$ and P2-Na_xRhO_2 phases

Figure 1 shows the X-ray powder diffraction pattern of the O3-$NaRhO_2$ phase obtained by solid state reaction along with a schematic representation of its structure. O3-$NaRhO_2$ was obtained as a brownish powder. Its X-ray powder diffraction pattern was analyzed and it was found to crystallize in the space group R-3m, with cell parameters similar to those already reported in the literature:[10] a= 3.0963(1) Å and c= 15.5251(1) Å. These cell parameters were determined from the profile refinement of the experimental data using Le Bail method.

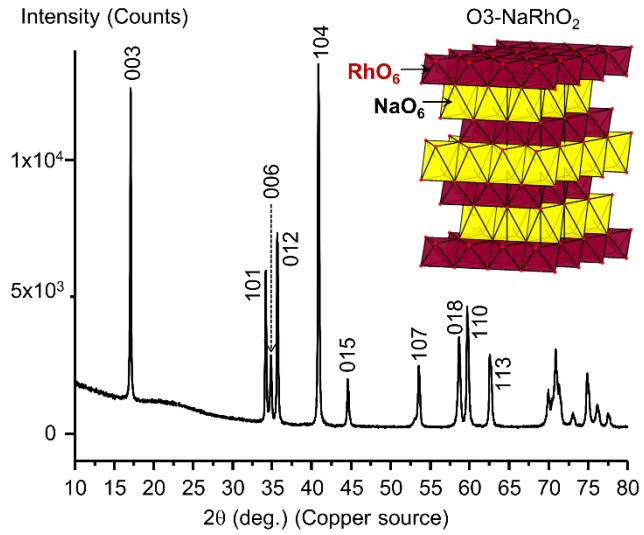

Figure 1. X-ray powder diffraction diagram recorded for O3-$NaRhO_2$. Indexation is given for using R-3m space group. A schematic representation of the O3-$NaRhO_2$ structure is given as an inset.

The synthesis of the P2-$Na_{0.70}RhO_2$ phase required two steps as described in the experimental section. Figure 2 shows in blue the X-ray powder diffraction pattern of the P2-$K_{0.62}RhO_2$ phase obtained after the first step of the synthesis. It can be indexed using the space group $P6_3/mmc$ with the following cell parameters: a=3.0670(1) Å and c = 12.2725(1) Å. The material was then used for the ion exchange reaction of potassium by sodium.

After the ion exchange reaction, an orange deposit appeared on the inner side of the glass tube. Moreover, the colorless acetonitrile solution became transparent yellow after having been used to wash the resulting powder. Therefore, we assumed that there was a redox reaction occurred and that iodine was formed during the ion exchange. In solution, the standard reduction potentials of I_2/I^- and Rh^{4+}/Rh^{3+} couples are 0.535 V and approximately 1.4 V vs the standard hydrogen electrode, respectively.[23] The following reaction could therefore be possible at the solid state:

$$Rh^{4+} + I^- \rightarrow Rh^{3+} + \frac{1}{2} I_2$$

The probable presence of iodine I_2 after the ion exchange reaction would involve the reduction of some Rh^{4+} ions in the P2-K_yRhO_2 phase in Rh^{3+} ions in the P2-Na_xRhO_2 phase. To balance the charges in the P2-Na_xRhO_2 phase, the amount of sodium ions intercalated within the P2-Na_xRhO_2 phase should be higher than that of potassium ions deintercalated from the P2-K_yRhO_2 phase. This is in agreement with the alkaline ion content found in both phases by electron microprobe, P2-$K_{0.62\pm0.03}RhO_2$ and P2-$Na_{0.70\pm0.03}RhO_2$.

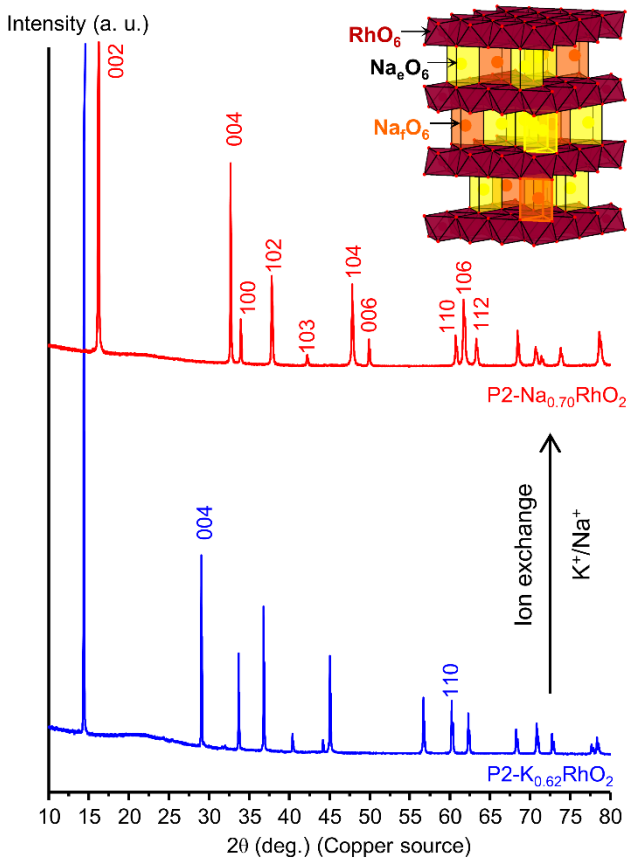

Figure 2. X-ray powder diffraction diagrams recorded P2-$Na_{0.70}RhO_2$ obtained by ion exchange from P2-$K_{0.62}RhO_2$ (top in red) and for P2-$K_{0.62}RhO_2$ (bottom in blue). Indexation is given for the main characteristic reflections for each compound using the space group $P6_3/mmc$. A schematic representation of the P2-$Na_{0.70}RhO_2$ structure is given as an inset at the top right corner.

After the ion exchange, the presence of sodium iodine NaI was detected by X-ray powder diffraction, indicating that no more Rh^{4+} ions could be reduced to Rh^{3+} ions even if some were still present in the P2-Na_xRhO_2 phase. An equilibrium was probably reached which was imposed by the reduction potential of the couple NaI/I_2. Moreover the cell parameters for the P2-Na_xRhO_2 phase calculated from the

X-ray diffraction patterns collected for different batches were all very similar indicating that ion exchange was a reproducible technique to synthesize the phase P2-$Na_{0.70}RhO_2$.

Figure 2 shows the X-ray powder diffraction patterns of the material before and after the ion exchange. The P2-type structure is notably preserved during the ion exchange reaction: after the ion exchange, the diffraction pattern of the P2-$Na_{0.70}RhO_2$ phase can still be indexed using the space group $P6_3/mmc$ with the following cell parameters: a=3.0474(1) Å and c=10.9584(1) Å. The decrease of the c parameter is consistent with the exchange of potassium by sodium in the P2-type structure, the ionic radius of potassium ion K^+ (1.38 Å) being larger than that of sodium ion Na^+ (1.02 Å). Only a small decrease of the a parameter is observed after the ion exchange as this parameter is constrained by in-plane Rh-Rh distances. No structure refinement using the Rietveld method was been performed to refine the structure of the new P2-type phase because the high value of the estimated absorption coefficient μR (approximately 5.5). For this high value of μR, corrections used by the Rietveld method are inaccurate. In P2-type structures, Na^+ ions usually occupy partially and randomly two different types of trigonal prismatic sites. One site shares edges with the RhO_6 octahedra (Na_eO_6 on Figure 2) whereas other one shares two faces with them (Na_fO_6 on Figure 2).

3.2. Electrochemical behavior of O3 and P2-Na_xRhO_2

Both materials, O3-$NaRhO_2$ and P2-$Na_{0.70}RhO_2$, were used as positive electrode materials in sodium batteries to explore the phase diagram of these two Na_xRhO_2 systems. Figure 3 shows the evolution of the cell voltage as a function of the sodium content *x* during the first galvanostastic cycle of batteries made with the O3-$NaRhO_2$ and P2-$Na_{0.70}RhO_2$ phases as positive electrode materials.

The electrochemical curve obtained for the O3-type phase is much more complex than the one published previously.[10] It shows plateaus and voltage steps, which suggests that several phase transitions occur during sodium electrochemical (de-)intercalation. During the first charge up to 3.8 V, sodium can be electrochemically de-intercalated to the composition $Na_{0.33}RhO_2$. On discharge, the electrochemical curve is very similar to that recorded on charge. However, there is a clear loss of capacity. This can be due to electrolyte degradation at high voltage: the electrolyte might oxidize during the charge at high voltage leading to an overestimation of the number of de-intercalated sodium ions. Although this liquid electrolyte was found to be stable in the 0-5 V window voltage range when aluminum was used as the working electrode,[24] we empirically observed that the electrochemical stability of liquid electrolytes actually depends on the nature of the transition metal ion present in the layered oxide used as the positive electrode. The loss in capacity on discharge could also be explained by the expected decrease in sodium conductivity for sodium content x close to 1 as a result of the decrease of divacancies.[25]

Two voltage steps are observed for compositions close to $Na_{1/2}RhO_2$ and $Na_{1/3}RhO_2$ indicating the existence of single phases with these chemical formulas. Theoretical and experimental studies have shown that for these specific compositions sodium ions tend to order between the $(MO_2)_n$ layers to minimize electrostatic repulsions.[3,26-28] Therefore, we believe that such orderings also exist in the O3-Na_xRhO_2 system.

The electrochemical curve obtained for the P2-type phase shows that the sodium electrochemical intercalation and de-intercalation is reversible in a narrower sodium content range than the O3-type phase, from $x \approx 0.8$ to $x \approx 0.4$. As for the battery made with the O3-type material, an important capacity irreversibility is observed on discharge probably due to the electrolyte degradation at high voltage. The electrochemical curve obtained for the battery made with the P2-$Na_{0.70}RhO_2$ phase at the positive electrode also shows discontinuities. A voltage step is also clearly observed for a composition close to $Na_{1/2}RhO_2$. Another one appears for a composition close to $Na_{2/3}RhO_2$. This indicates the existence of single phases with these two chemical formulas. Other smooth voltage drops are visible at approximately 2.85 V and 3.75 V suggesting that other single phases could be found in the P2-Na_xRhO_2 with different sodium/vacancy orderings.

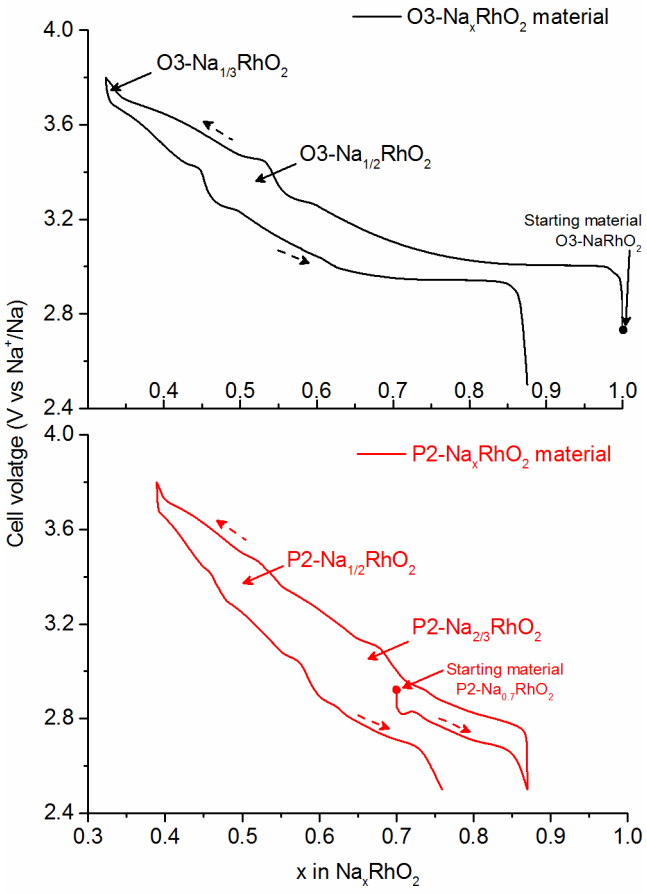

Figure 3. Evolution of cell voltage as a function of the sodium content of sodium batteries made of O3-$NaRhO_2$ (top in black) and of P2-$Na_{0.70}RhO_2$ (bottom in red) cycled between 2.5 V and 3.8 V.

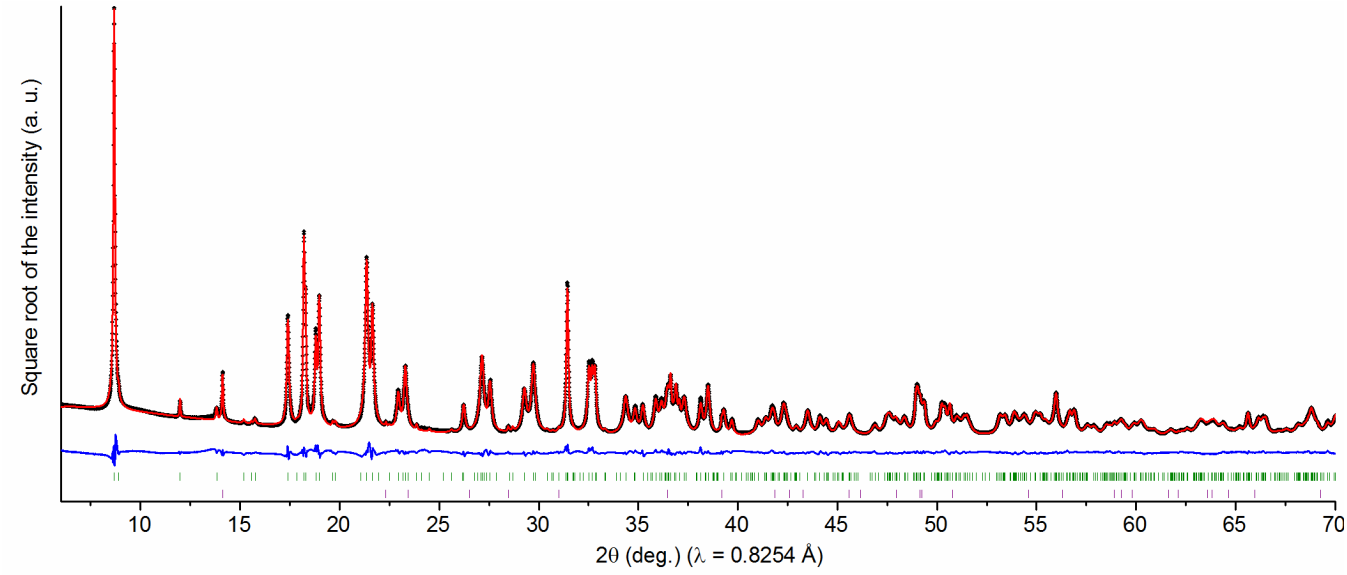

Figure 4. Experimental high resolution X-ray powder diffraction pattern of O'3-$Na_{1/2}RhO_2$ (black diamonds), calculated pattern obtained from the Rietveld refinement (red line) and difference line (blue line). Green and purple bars show the position of the Bragg reflections for O'3-$Na_{1/2}RhO_2$ and graphite, respectively.

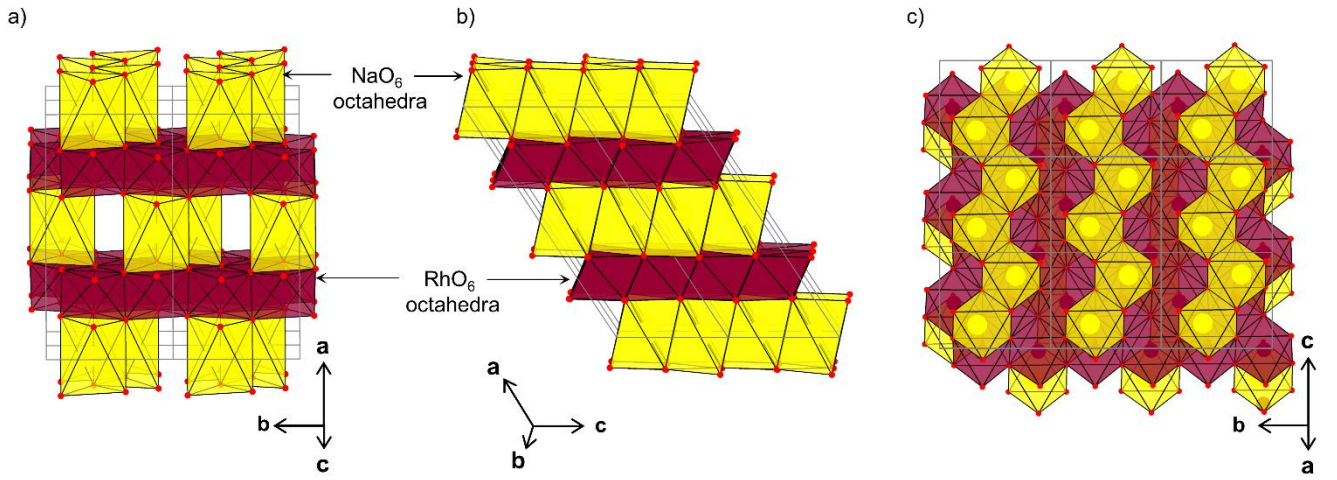

Figure 5. Structure of O'3-$Na_{1/2}RhO_2$. Three-dimensional overviews (a and b) and projection parallel to the $(RhO_2)_n$ layers (c). Limits of the unit cells are shown in grey.

3.3. Electrochemical synthesis of the O'3-$Na_{1/2}RhO_2$ phase

The electrochemical curves obtained for batteries made with the O3-$NaRhO_2$ and P2-$Na_{0.70}RhO_2$ phases at the positive electrode suggest that single phases showing sodium ordering exist with specific compositions in these two systems. To confirm this hypothesis, we chose to synthesize electrochemically the phase $Na_{1/2}RhO_2$ in the O3-type system.

High resolution X-ray powder diffraction data collected for this phase are presented in Figure 4. This X-ray diffraction pattern cannot be indexed using the space group R-3m which is used to index X-ray diffraction pattern of the pristine material O3-$NaRhO_2$. Firstly, there are extra peaks in the 2θ-range 9.5 - 17 °, which corresponds to a 2θ-range of 17 - 32 ° for a pattern recorded with a conventional X-ray source operating with copper. The presence of these peaks usually indicates that a larger cell should be used to index properly the diffraction pattern of $Na_{1/2}RhO_2$. Secondly, some peaks are split indicating that the hexagonal symmetry is lost and that a monoclinic cell should be used to index the pattern.

Therefore, the structural model proposed for O'3-$Na_{1/2}VO_2$, obtained from electrochemical deintercalation from O3-$NaVO_2$,[29] was used to index the X-ray diffraction of O'3-$Na_{1/2}RhO_2$. The distorted structure is called O'3 (the symbol " ' " indicates the occurrence of a structural distortion of the hexagonal lattice).[14] The structure was refined using the Rietveld method starting from the structural model proposed for O'3-$Na_{1/2}VO_2$. It lead to a good fit of the experimental data with very good reliability factor (Weighted-profile *R*-factor R_{wp} = 5.60 %, goodness of fit GoF = 7.83). The cell parameters and the atomic positions

are given in Table 1. A representation of the structure of O'3-$Na_{1/2}RhO_2$ is given in Figure 5. It shows that sodium remains in octahedral sites and it confirms that sodium ions order to form infinite zig-zag chains along the c-axis. The triangular lattice formed by rhodium remains regular with homogeneous Rh-Rh distances comprised between 3.019 Å and 3.060 Å. In O'3-$Na_{1/2}VO_2$, there is a distribution of V-V distances which are comprised between 2.64 Å to 3.01 Å due to the formation of shorts V-V bonds. In the case of O'3-$Na_{1/2}RhO_2$, the presence of low spin $4d^5$ and $4d^6$ ions is not favorable to the formation of shorts Rh-Rh bonds. Therefore the monoclinic distortion is due to the sodium ordering and not to transition metal clustering like in O'3-$Na_{1/2}VO_2$.

For O'3-$Na_{1/2}VO_2$, the O3-type structure was metastable and it was possible to induce the slab gliding to generate a P3-type structure by heating the material at 100 °C. The O3-type stacking was found to be stable in $Na_{1/2}RhO_2$ and no gliding was observed up to 300 °C.

Table 1. Refined atomic positions and atomic displacement parameters (B_{iso}) in O'3-$Na_{1/2}VO_2$ at 300 K in the monoclinic unit cell a=13.1020(2) Å, b=6.0905(1) Å, c=5.2788(2) Å, β=123.627(2)° and the space-group *C*2/*c*. Weighted-profile *R*-factor R_{wp} = 5.60 %, Goodness of fit GoF = 7.83.

Atom	Wyckoff position	x	y	z	B_{iso} (Å²)
Rh	8f	0.2486(3)	0.3737(2)	0.2476(3)	0.25(1)
Na	4e	0	0.329(2)	1/4	1.74(5)
O1	8f	0.352(1)	0.122(1)	0.225(1)	0.34(2)
O2	8f	0.165(1)	0.114(1)	0.297(1)	0.34(2)

3.4. Electrical properties of O3-NaRhO2 and O'3-$Na_{1/2}RhO_2$

Electrical resistivity measurements on O3-$NaRhO_2$ and O'3-$Na_{1/2}RhO_2$ are plotted on Figure 6. The resistivity of O3-$NaRhO_2$ shows a semiconductor behavior with a decrease of the resistivity when the temperature increases.

Figure 6(c) shows the variation of Naperian logarithm of the electrical conductivity as a function of T^{-1} (Arrhenius equation). Between 130 K and 290 K, a linear variation is observed corresponding an activation energy $E_a \approx 0.46$ eV, which is in agreement with values usually observed for a hopping conduction mechanism. However a significant discrepancy is observed at lower temperatures down to 100 K. Therefore, we used the variable range hopping (VRH) model instead to fit the experimental data.[30]

As shown in Figure 6(d), the variation of Naperian logarithm of the electric conductivity as a function of $T^{-1/4}$ is fairly linear. This VRH behavior might be related to a localization of the electrons; however additional transport property measurements are required in order to understand the interactions at the origin of this behavior.

On the opposite, the resistivity of O'3-$Na_{1/2}RhO_2$ increases when the temperature increases indicating that the phase is metallic. This could be due to the presence within the $(RhO_2)_n$ layers of a mix valence state for rhodium, i.e. a mixture of Rh^{3+} and Rh^{4+} ions. This metallic behavior was observed for Na_xRhO_2 single crystals for $x < 0.5$ and it was attributed to the transport of hole carriers.[16]

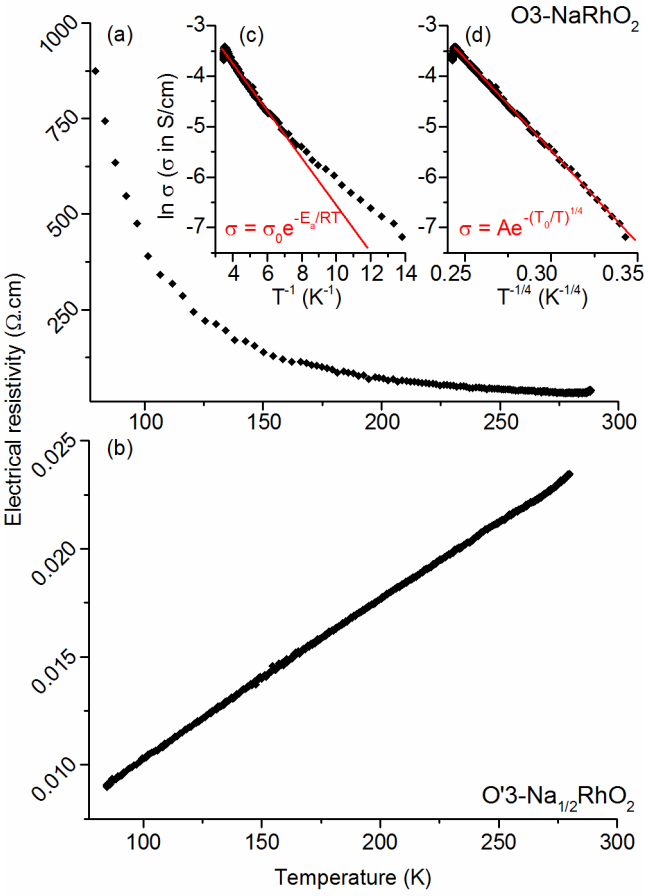

Figure 6. Electrical resistivity measured on pellets of (a) O3-$NaRhO_2$ and (b) O'3-$Na_{1/2}RhO_2$. The insets show the linear regression of the Naperian logarithm of the electrical conductivity σ with different models for O3-$NaRhO_2$, : (c) Arrhenius law with a T^{-1} dependence (fitted in the 280–1 temperature range, $R^2 = 0.962$) and (d) variable range hopping with a $T^{-1/4}$ dependence (fitted in the 280–80 K temperature range, $R^2 = 0.985$).

CONCLUSION

Phases in the Na_xRhO_2 layered system were obtained with both O3- and P2-type structures. Whereas the synthesis of O3-$NaRhO_2$ had already been reported in the literature, P2-$Na_{0.7}RhO_2$ phase was synthesized for the first time by ion exchange from P2-$K_{0.62}RhO_2$. This type of synthesis could be implemented on other systems to obtain new P2-type phases with 3d or 4d transition metal ions.

The investigation of the phase diagram by sodium electrochemical (de-)intercalation of the O3-Na_xRhO_2 system revealed a reversibility in the 0.33 < x < 1 range, with a loss in capacity presumably due to the electrolyte decomposition at high voltage. Two voltage steps were observed on the electrochemical curve and they suggested the existence of two single phases with specific composition in the system: $Na_{1/2}RhO_2$ and $Na_{1/3}RhO_2$. O'3-$Na_{1/2}RhO_2$ was electrochemically synthesized and its structure was solved by high resolution X-ray Powder diffraction. It exhibits a monoclinic distortion which is due to the sodium ordering between the $(RhO_2)_n$ layers. Interestingly, O'3-$Na_{1/2}RhO_2$ has a metallic behavior, whereas O3-$NaRhO_2$ is semi-conducting. Further detailed characterizations of the Seebeck coefficient and the thermal conductivity need to be performed on O'3-$Na_{1/2}RhO_2$ to probe its thermoelectric figure of merit.

The range of reversibility of sodium electrochemical (de-)intercalation for the P2-Na_xRhO_2 system is narrower, 0.4 < x < 0.8. Voltage steps were also observed on the electrochemical curve and they suggested the existence several phases in the system, including P2-$Na_{1/2}RhO_2$. This work provides a first insight of the variety of phases which can be obtained in the Na_xRhO_2 system. The P2-type phases are the most promising candidates for thermoelectric properties, as it was demonstrated on cobalt layered oxides.

AUTHOR INFORMATION

Corresponding Author

* Email: marie.guignard@icmcb.cnrs.fr

Present Addresses

†Department of Materials Science and Engineering, Drexel University, Philadelphia PA, United States

Author Contributions

The manuscript was written through contributions of all authors. All authors have given approval to the final version of the manuscript.

Funding Sources

This work was supported by the Agence Nationale de la Recherche through the grant ANR-14-CE05-0011.

ACKNOWLEDGMENT

Authors are grateful to T. Renzi, T. Broux and F. Fauth for their help for the high resolution X-ray powder diffraction data collection at the Materials Science and Powder Diffraction (BL04-MSPD) beamline at Alba synchrotron. The authors thank R. Decourt for transport measurements, C. Denage and E. Guérin for assistance.

REFERENCES

(1) Takada, K.; Sakurai, H.; Takayama-Muromachi, E.; Izumi, F.; Dilanian, R. A.; Sasaki, T. Superconductivity in Two-Dimensional CoO2 Layers. *Nature* **2003**, *422 (6927)*, 53–55.

(2) Molenda, J.; Delmas, C.; Hagenmuller, P. Electronic and Electrochemical Properties of Na_xCoO_{2-y} Cathode. *Solid State Ion.* **1983**, *9 & 10 (1)*, 431–436. Terasaki, I.; Sasago, Y.; Uchinokura, K. Large Thermoelectric Power in NaCo2O4 Single Crystals. *Phys. Rev. B* **1997**, *56 (20)*, R12685–R12687.

(3) Huang, Q.; Foo, M. L.; Lynn, J. W.; Zandbergen, H. W.; Lawes, G.; Wang, Y.; Toby, B. H.; Ramirez, A. P.; Ong, N. P.; Cava, R. J. Low Temperature Phase Transitions and Crystal Structure of $Na_{0.5}CoO_2$. *J. Phys. Condens. Matter* **2004**, *16 (32)*, 5803–5814.
Meyer, G.; Hoppe, R. Über Oxoniobate (III). II [1, 2]. Notiz zur Kenntnis von $NaNbO_2$. *Z. Anorg. Allg. Chem.* **1976**, *424 (2)*, 128–132.

(4) Ringenbach, C.; Kessler, H.; Hatterer. A. Un Nouveau Composé Oxygéné du Molybdène $NaMoO_2$. Propriétés Cristallographiques et Magnétiques. *C. R. Acad. Sc. Paris, Série C* **1969**, *269*, 1394–1397.

(5) Réau, J.-M.; Fouassier, C.; Hagenmuller, P. Les Systèmes MoO_2-A_2O et WO_2 -A_2O (A = Li, Na, K). *Bull. Soc. Chim. Fr.*, **1970**, *11*, 3827–3829.

(6) Shikano, M.; Delmas, C.; Darriet. J. $NaRuO_2$ and Na_xRuO_2 .yH_2O: New Oxide and Oxyhydrate with Two Dimensional RuO_2 Layers. *Inorg. Chem.* **2004**, *43 (4)*, 1214–1216.

(7) Scheer, J. J.; Van Arkel, A. E.; Heyding. R. D. Oxide Complexes Formed in the Systems Platinum Metals : Alkali Carbonates : Oxygen. *Can. J. Chem.* **1955**, *33 (4)*, 683–686.

(8) Chang, S. O.; Park, H.-H., Maazaz, A.; Delmas, C. Sur l'Obtention des Oxydes Lamellaires $LiNbO_2$et $NaNbO_2$ par Voie Chimique et Electrochimique. Préparation par Désintercalation des Solutions Solides Correspondantes. *C. R. Acad. Sc. Paris, Série II* **1989**, *308*, 475–478.

(9) Tarascon, J. M.; Hull, G. W. Sodium Intercalation into the Layer Oxides $NaMo_2O_4$. *Solid State Ion.* **1986**, 22 (1), 85–96.

(10) Mendiboure, A.; Eickenbusch, H.; Schöllhorn, R.; Rao, G. V. S. Layered Alkali Rhodium Oxides A_xRhO_2: Topotactic Solvation, Exchange, and Redox Reactions. *J. Solid State Chem.* **1987**, *71 (1)*, 19–28.

(11) Rzeznik, M. A.; Geselbracht, M. J.; Thompson, M. S.; Stacy, A. M. Superconductivity and Phase Separation in Na_xNbO_2 (x < l). *Angew. Chem.-Int. Edit.* **1993**, *32 (2)*, 254–255.

(12) Saeed, Y.; Singh, N.; Schwingenschlögl, U. Superior Thermoelectric Response in the 3R Phases of Hydrated Na_xRhO_2. *Sci Rep* **2014**, *4*, 4390-1–4390-4.

(13) Hobbie, K.; Hoppe, R. Zum Aufbau von $NaRhO_2$. *Z. Anorg. Allg. Chem.* 1988, 565, 106–110.

(14) Delmas, C.; Fouassier, C.; Hagenmuller P. Structural Classification and Properties of the Layered Oxides. *Physica B + C* **1980**, *99 (1–4)*, 81–85.

(15) Varela, A.; Parras, M.; Gonzalez-Calbet, J. M. Influence of Na Content on the Chemical Stability of Nanometric Layered Na_xRhO_2 ($0.7 \le x \le 1.0$). *Eur. J. Inorg. Chem.* **2005**, *2005 (21)*, 4410–4416.

(16) Zhang, B.-B.; Wang, C.; Dong, S.-T.; Lv, Y.-Y.; Zhang, L.; Xu, Y.; Chen, Y. B.; Zhou, J.; Yao, S.-H.; Chen, Y.-F. Preparation, Structure Evolution, and Metal–Insulator Transition of Na_xRhO_2 Crystals ($0.25 \le x \le 1$). *Inorg. Chem.* **2018**, *57 (5)*, 2730–2735.

(17) Delmas, C.; Braconnier, J.-J.; Fouassier, C.; Hagenmuller, P. Electrochemical Intercalation of Sodium in Na_xCoO_2 Bronzes. *Solid State Ionics* **1981**, *3–4*, 165–169.

(18) Braconnier, J.-J.; Delmas, C.; Hagenmuller, P. Etude par Désintercalation Electrochimique des Systèmes Na_xCrO_2 et Na_xNiO_2. *Mater. Res. Bull.* **1982**, *17 (8)*, 993–1000.

(19) Komaba, S.; Nakayama, T.; Ogata, A.; Shimizu, T.; Takei, C.; Takada, S.; Hokura, A.; Nakai, I. Electrochemically Reversible Sodium Intercalation of Layered $NaNi_{0.5}Mn_{0.5}O_2$ and $NaCrO_2$. *ECS Trans.* **2009**, *16 (42)*, 43–55.
(20) Han, M. H.; Gonzalo, E.; Casas-Cabanas, M.; Rojo, T. Structural Evolution and Electrochemistry of Monoclinic $NaNiO_2$ upon the First Cycling Process. *J. Power Sources* **2014**, *258*, 266–271.
(21) Guignard, M.; Dider, C.; Darriet, J.; Bordet, P.; Elkaïm, E.; Delmas, C. P2-Na_xVO_2 system as electrodes for batteries and electron-correlated materials. *Nat. Mater.* **2013**, *12*, 74–80.
(22) Yubuta, K.; Shibasaki, S.; Terasaki, I.; Kajitani, T. High-resolution electron microscopy for incommensurate structure of K_xRhO_2 crystal. *Philos. Mag.* **2009**, *89 (31)*, 2813–2833.
(23) Bratsch, S. J. Standard Electrode Potentials and Temperature Coefficients in Water at 298.15 K. *J. Phys. Chem. Ref. Data* **1989**, *18 (1)*, 1–21.
(24) Ponrouch, A.; Marchante, E.; Courty, M.; Tarascon, J.-M.; Palacin, R. M. In search of an optimized electrolyte for Na-ion batteries. *Energy Environ. Sci.*, **2012**, *5*, 8572–8583.
(25) Mo, Y.; Ong, S. P.; Ceder, G. Insights into Diffusion Mechanisms in P2 Layered Oxide Materials by First-Principles Calculations. *Chem. Mater.* **2014**, *26 (18)*, 5208–5214.
(26) Meng, Y. S.; Hinuma, Y.; Ceder, G. An Investigation of the Sodium Patterning in Na_xCoO_2 ($0.5 \leq x \leq 1$) by Density Functional Theory Methods. *J. Chem. Phys.* **2008**, *128*, 104708.
(27) Wang, Y.; Ding, Y.; Ni, J. Ground-State Phase Diagram of Na_xCoO_2: Correlation of Na Ordering with CoO2 Stacking Sequences. J. *Phys.: Condens. Matter* **2009**, *21*, 035401.
(28) Toumar, A. J.; Ong, S. P. ; Richards, W. D. ; Dacek, S.; Ceder, G. Vacancy Ordering in O3-Type Layered Metal Oxide Sodium-Ion Battery Cathodes. *Phys. Rev. Appl.* **2015**, *4 (6)*, 064002**.**
(29) Didier, C.; Guignard, M.; Darriet, J.; Delmas, C. O'3-Na_xVO_2 system: a superstructure for $Na_{1/2}VO_2$. *Inorg. Chem.* **2012,** *51 (20)*, 11007–16.
(30) Mott, N. F. Conduction in non-crystalline materials. *Philos. Mag.* **1969**, 19, 835–852.

TOC

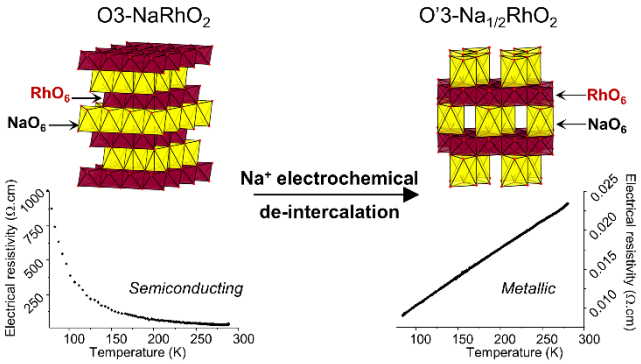

O'3-$Na_{1/2}RhO_2$ is one of the many phases that could be obtained in the Na_xRhO_2 systems by sodium electrochemical de-intercalation in a sodium battery. The change in the sodium content in the layered oxide results in the modification of its electronic properties, from a semiconducting behavior in O3-$NaRhO_2$ to a metallic one in O'3-$Na_{1/2}RhO_2$.